Journal of Electrical and Computer Engineering Innovations
(JECEI)
Journal homepage: http://www.jecei.sru.ac.ir

Research paper

A SOGI-PLL-Based Feedback-Feedforward Control System for Three-Phase Dynamic Voltage Restorer in the Distribution Grid

R. Nasrollahi[1], H. Feshki Farahani[2,*], M. Asadi[3], M. Farhadi-kangarlu[4], P. Amiri[5]

[1]*Department of Electrical Engineering, Central Tehran Branch, Islamic Azad University, Tehran, Iran.*

[2]*Department of Electrical and Computer Engineering, Ashtian Branch, Islamic Azad University, Ashtian, Iran.*

[3]*Faculty of Electrical and Computer Engineering, Arak University of Technology, Arak, Iran.*

[4]*Faculty of Electrical and Computer Engineering, Urmia University, Urmia, Iran.*

[5]*Faculty of Electrical Engineering, Shahid Rajaee Teacher Training University, Tehran, Iran.*

Article Info

Article History:
Received 10 February 2021
Reviewed 23 March 2021
Revised 29 May 2021
Accepted 17 June 2021

Keywords:
Dynamic voltage restorer
Power quality
Sensitive load
AC/AC converter
Combined feedback and feedforward control

[*]Corresponding Author's Email Address:
hfeshki@aiau.ac.ir

Abstract

Background and Objectives: Due to the increased sensitive loads, improving power quality in distribution grids by custom power tools is one of the important fields of electrical engineering. This paper proposes a new kind of three-phase three-wire dynamic voltage restorer (without including storage sources or DC link) and also its control method.
Methods: The proposed structure includes an AC/AC converter, low-pass filters at the input and output sides, and three-phase injection transformers. The control system is based on the combination of feedback and feedforward control that its advantages are high speed, good response quality, and very simple implementation. To overcome the harmonics raised from AC/AC converter switching on the main line, a SOGI-PLL has been used. Also, SOGI-PLL operates independently on each phase so that the asymmetric voltage variations can be identified.
Results: The proposed control method is capable to compensate the power quality problems such as voltage sag, swell, and harmonics in balanced and unbalanced conditions. The detailed modelling and design of the proposed controller are verified through computer simulations and experimental results under different operating conditions. Simulation and experimental results show that the proposed control strategy can compensate the power quality events as close as possible to the desired values under different operation modes.
Conclusion: In this paper, a three-phase three-wire dynamic voltage restorer (DVR) was assessed using direct AC/AC converters without a supply source and DC link. A control system based on combined feedback and feedforward control (CFBFFC) and SOGI-PLL has been proposed for the DVR. The simulation results on a three-phase 20kV system as well as the experimental results obtained from a single-phase 220V system verified the performance of the DVR and the control system. It was shown that this structure can compensate for 0.5pu voltage sag, above 1pu voltage swell, and all kinds of harmonic faults.

Introduction

At the distribution grid, power quality (PQ) problems occur for a variety of reasons including power system faults, nonlinear loads, large loads switching, and high-power induction motor drives [1].

It should be noted that due to the very high expansion of renewable energy resources and electric vehicles in the future, the problems related to the PQ can be very significant [2], [3], [4], [5], [6], [7].

Custom power devices are powerful tools based on the semiconductor switches used for protecting sensitive loads and solving PQ issues in the distribution system [8], [9], [10], [11]. In power systems, the voltage sag and voltage swell are the most common failures, and according to Electric Power Research Institute (EPRI) estimates, they account for about 87% of faults [12], [13].

DVR is one of the most effective, efficient, and economic custom power devices used in power distribution systems that can protect sensitive loads against PQ problems by injecting proper voltage in series during disturbance time [14], [15]. DVR has several structures and usually, a supply source or DC link is used in its structure. Removing the DC link from the DVR structure causes significant decreases in its volume and weight. As shown in Fig. 1, most of the power component problems during operation are related to the use of DC-link capacitors (diagram values can vary in different circuits), so by removing them, the relevant problems will be eliminated [15], [16].

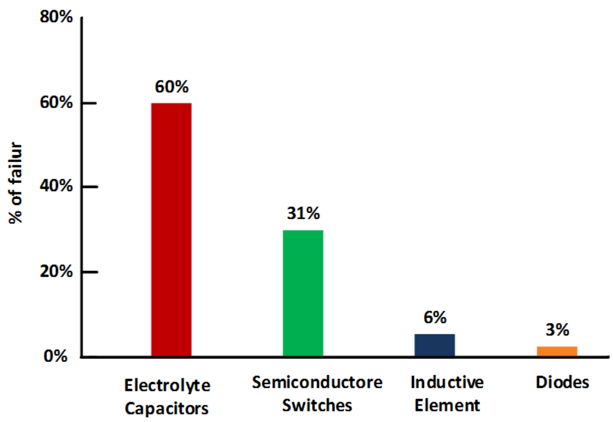

Fig. 1: Distribution of power component failure [16].

In recent years, several control strategies have been developed for DVR control, some of which include: neural network control [17], predictive control [18], fuzzy control [19], repetitive control [20], and sliding mode control [21], [22]. In addition to the advantages, each of the above methods has its disadvantages, such as dependence on the model and sensitivity to parameter changes, but there are drawbacks to the complexity of implementation in all of them. In the industry, simple linear controllers are mostly used due to their easy structure and implementation and proper operation of these controllers. System simplicity and low complexity of implementation in the industry is very important and has several advantages, so in this article, the simple PI feedback control method is combined with the feedforward control and using it, the optimal response to compensate voltage sag, voltage swell and harmonic problems has been created in the distribution network. This method has several advantages, including high response speed due to the use of feed-forward control in the controller structure, good response quality according to the output results, Ease of implementation due to the controller structure, and removal of voltage source harmonics at the output. As a summary of the literature review, it can be concluded that various structures and control methods have been presented for DVR in the literature. The AC-AC converter-based DVRs do not require energy storage or DC-link capacitors which reduces the volume, weight and, failure of DVR [15], [16], [23]. On the other hand, the combined feedback and feedforward control (CFBFFC) method has some advantages that are already mentioned [24], [25]. The CFBFFC application in AC-AC converter-based DVR has not been presented in the literature which is investigated in this paper. The novelties of this paper can be summarized as follows:

- combined feedback and feed-forward control of the AC-AC converter-based DVR
- SOGI-PLL is used to suppress the effect of grid voltage harmonics on the control performance
- In addition to compensating the voltage sags and voltage swells, it is also able to eliminate the source harmonic voltages on the load terminals

This paper is organized in the following sequence. First, the structure of the DVR system including general structure and compensation capability, operation of the converter, and control system are described. In the next section, simulation and experimental results are shown and in the last section, the conclusion of the article is presented.

Structure and Control System of Dynamic Voltage Restorer

A. General Structure and Compensation Capability

Fig. 2a shows a three-phase three-wire network including a DVR and its detailed structure is depicted in Fig. 2b. The overall structure of the DVR consists of an input filter, PWM AC-AC converter, output filter, and injection transformer.

The AC-AC converter includes four bidirectional switches in each phase that acts as a buck converter [26]. It generates an output voltage with a desirable phase angle, therefore, it can compensate the voltage sag as well as voltage swell. Also, as three independent units are used, the asymmetric voltage sag and swell can be compensated. The real application of DVR is usually located at the medium voltage (20kV) distribution lines where the ground wire of the network is not usually accessible, so for the correct operation of the circuit, a neutral point is created as shown in Fig. 2b.

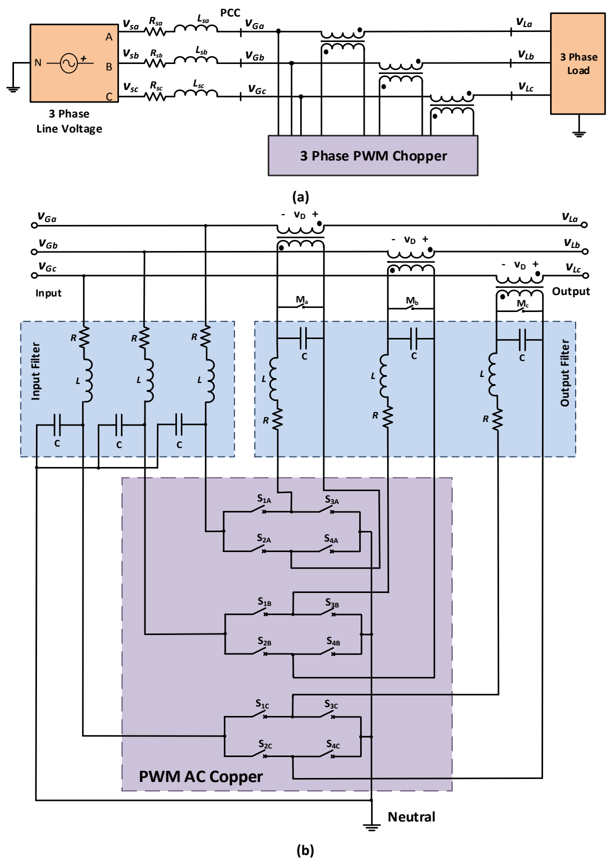

Fig. 2: DVR structure with AC-AC converter and input and output filters.

Due to not requiring energy storage, the compensation time is not limited as in the conventional DVR with energy storage. However, in the AC-AC converter-based compensators, the current increase from the grid for compensation would reduce the grid voltage by itself, which can cause problems in weak grids [27]. Because the proposed DVR uses the grid-connected AC-AC converter and generates the compensating voltage using the grid voltage, the maximum value of the DVR output voltage magnitude will depend on the grid voltage as well as the transformer turns ratio. Based on Fig. 2 and neglecting the voltage drop on the input and output filters and the injection transformer, the following equation can be written:

$$V_D = nDV_G \tag{1}$$

where, V_D and V_G are the magnitude of the DVR output voltage and that of the grid voltage, respectively. Also, n is the transformer turns ratio defined as the ratio of the number of grid-side turns to that of the converter-side. D is the converter duty cycle that will be discussed later.

Considering that the DVR output voltage is in-phase with the grid voltage, (2) can be written:

$$V_L = V_G + V_D \tag{2}$$

Using (1) and (2), the following equation is obtained:

$$V_L = 1 + nD\ V_G \tag{3}$$

Equation (3) can be manipulated as (4):

$$\frac{V_G}{V_L} = \frac{1}{1+nD} \tag{4}$$

If the DVR operates successfully, V_L is equal to its nominal value. Therefore, taking it as the voltage base value, (4) can be rewritten as (5) in per-unit (pu):

$$V_{G,pu} = \frac{1}{1+nD} \tag{5}$$

The voltage sag can be defined as $V_{sag,pu}=1-V_{G,pu}$. Based on this definition, (5) can be manipulated as (6):

$$V_{Sag,pu} = \frac{nD}{1+nD} \tag{6}$$

Considering that the maximum value of D is 1, the maximum value of the voltage sag that can be compensated by the DVR ($V_{sag,pu,\,max}$) is achieved by (7):

$$V_{Sag,pu,max} = \frac{n}{1+n} \tag{7}$$

For example, if the turn ratio is 1, the DVR will be able to compensate for up to 0.5pu voltage sag. By increasing n, more compensation can also be possible.

Also, for the voltage swell, $V_L = 1 - nD\ V_G$ and $V_{swell,pu} = V_{G,pu} - 1$, so the equation (8) is obtained:

$$V_{Swell,pu} = \frac{nD}{1-nD} \tag{8}$$

In this equation, if the turns ratio is 1 and *D* is 0.5 the DVR will be able to compensate for up to 1pu voltage swell, and if $0.5 < D < 1$, compensation more than 1pu can be obtained.

B. Operation of the converter

To demonstrate the performance of the AC-AC converter, the single-phase representation of the DVR is illustrated in Fig. 3. The converter consists of bidirectional switches as shown in the figure. Different configurations can be used for bidirectional switches, however, two common-emitter IGBTs are used as a bidirectional switch in this paper. At the input side of the converter, a low-pass LC filter is used to mitigate the high-frequency harmonics of the converter flowing to the grid. Also, another low-pass LC filter is used at the output side of the converter to filter out the high-frequency switching harmonics of the output voltage.

The filtered output voltage is injected into the grid via single-phase transformers. If the input voltage is within the normal range, the switches are not operated and the DVR is bypassed through the bypass switch (M_a). When a voltage disturbance (voltage sag and voltage swell) is detected, the bypass switch is opened and the converter is controlled in a way that the required compensation voltage is generated and injected into the grid. The detailed structure of the DVR in a single phase is illustrated in Fig. 3.

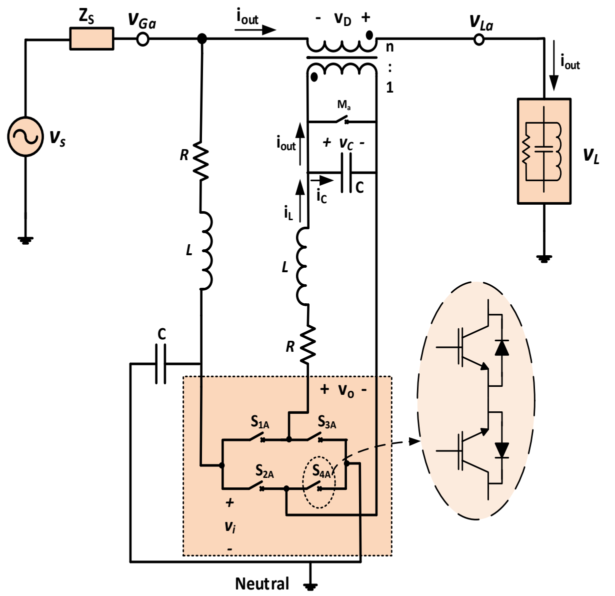

Fig. 3: Single-phase DVR structure with AC-AC converter.

The AC-AC converter used in each phase has four switches denoted as S_{1A}, S_{2A}, S_{3A}, and S_{4A}. The switching table of the converter is shown in Table 1. The switching combinations S_{1A} (or S_{3A}) and S_{4A} are used to generate the output voltage in-phase with the input voltage and hence compensating the voltage sag. To generate the output voltage with the opposite phase concerning the input voltage (and hence compensation for voltage swell) the switching combinations S_{2A} and S_{3A} (or S_{1A}) are used. The typical operation of the converter in this case is indicated in Fig. 4. The figure shows the converter input voltage (v_i), output voltage (v_o), and the averaged (or filtered) output voltage (v_c).

Fig. 4a shows the voltage sag compensation operation. As the figure illustrates, the converter output voltage is a switched voltage between the input voltage and the zero voltage level.

Fig. 4b shows the magnified view of the waveforms. As the figure indicates, in the time interval T_1 the switches S_{1A} and S_{4A} are turned on and the output voltage is equal to the input voltage.

Also, in the time interval T_2 the switches S_{3A} and S_{4A} are turned on and the output voltage is zero.

It should be noted that $T=T_1+T_2$ is the switching period which can be written as $T=1/f_s$, where fs is the switching frequency. If the duty cycle of the converter is defined as $D=T_1/T$, the average value of the converter output voltage in each switching period $(\bar{v}_o)$ can be written as follows:

$$\bar{v}_o = Dv_i \tag{9}$$

If the voltage drop on the input and output filters are neglected ($\bar{v}_o \cong v_C, v_i \cong v_G$) then the following equation can be written:

$$v_C = Dv_G \tag{10}$$

Equation (10) suggests that to generate the desired compensation voltage, the duty cycle should be obtained. In other words, the reference value of the duty cycle (D*) can be obtained as follows:

$$D^* = \frac{v_C^*}{v_G} \tag{11}$$

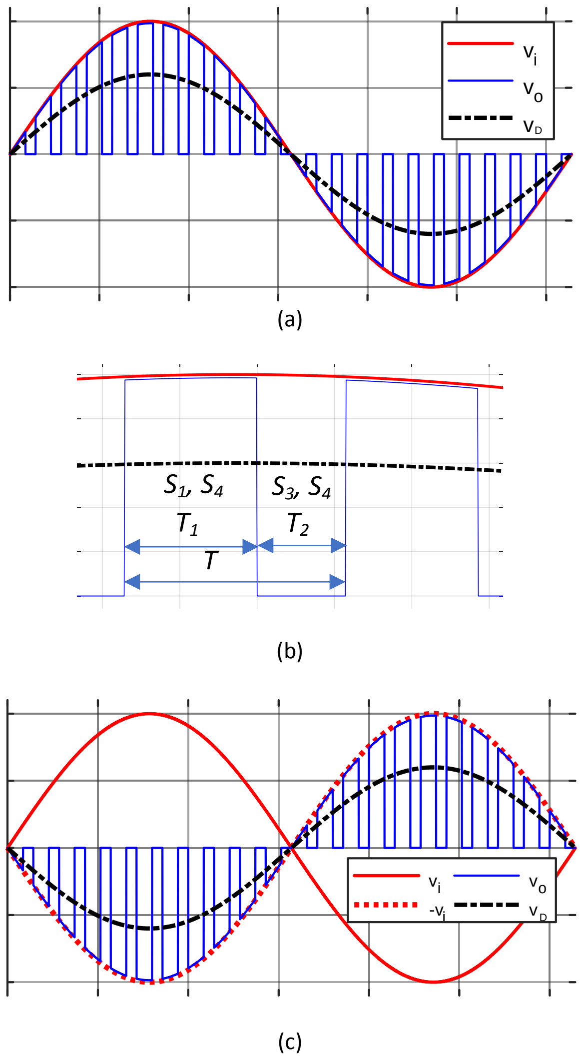

Fig. 4: Operation of the AC-AC converter, (a) voltage sag compensation, (b) magnified view, (c) voltage swell operation.

The operation of the converter in the case of voltage swell operation is similar to that of voltage sag compensation. However, as indicated in Fig. 4c, in the case of a voltage swell the output voltage is obtained by switching between $-v_i$ and zero.

Table 1: Switching table of the AC-AC converter

No	ON switches	Output voltage(v_L)
1	S_{1A}, S_{2A}	0
2	S_{3A}, S_{4A}	0
3	S_{1A}, S_{4A}	$+v_i$
4	S_{2A}, S_{3A}	$-v_i$

C. Control System

The simple method of execution and high response speed can be an important advantage in the design of the controller, so in this paper, a combination of feed-forward control with PI feedback control is used. To control the circuit, a feedforward structure is used for high-performance speed since the DVR is usually located between the grid and the load and is supposed to compensate for the grid fault. To completely control the slight error in the output or to compensate for the faults due to load variation, a feedback structure with a PI controller is placed to eliminate the existing fault. The PI controller coefficients are Ki=0.7 and Kp=1 and are regulated manually. According to the advantages icluding fast dynamic responses, ease to implement, optimal output quality, and removal of voltage source harmonics at the output and therefore in this research, this control method has been used.

The overall controller structure is shown in Fig. 5. As shown in the figure, phase-locked loop (PLL) based on quadratic signal generation (SOGI) quadratic signal generation (QSG) is used for various purposes. The SOGI conversion functions are as following [28]:

$$F_1(s) = \frac{v_{G,\alpha}}{v_G}(s) = \frac{K\omega s}{s^2 + K\omega s + \omega^2} \tag{12}$$

and

$$F_2(s) = \frac{v_{G,\beta}}{v_G}(s) = \frac{K\omega^2}{s^2 + K\omega s + \omega^2} \tag{13}$$

where ω is the angular velocity of the source voltage, and K is the damping coefficient of the algorithm. In [28] for system analysis, the Bode plot was evaluated, in which for relations (12) and (13), the value of K=1 and ω=100π(rad/s) were considered. Using the Bode plot presented $F_1(s)$ is a band-pass filter (BPF) and $F_2(s)$ is also a low-pass filter (LPF), hence it can be said that the SOGI is an adaptive filter that is very effective in harmonic contaminated systems [28], [29].

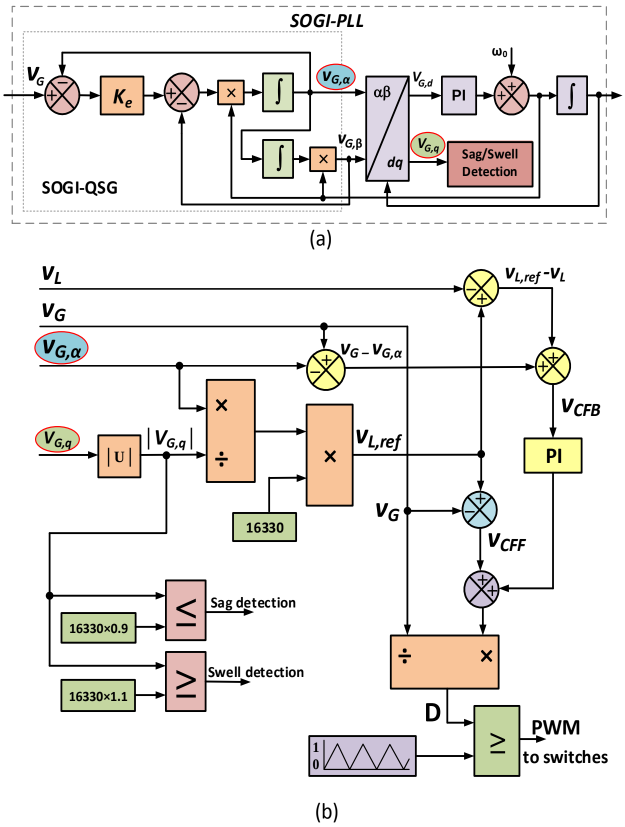

Fig. 5: CFBFF control structure with SOGI-PLL [27].

The SOGI-QSG generates the two quadrature signals from the input grid voltage, one is in-phase with the grid voltage, $v_{G,\alpha}$, and the other is in-quadrature with it, $v_{G,\beta}$ [27]. It is important to note that if the grid voltage signal contains harmonics, the SOGI-QSG will remove them so that $v_{G,\alpha}$ will be without the harmonics. The quadrature signals are then in the PLL to extract the phase angle of the grid voltage as well as the dq component of it, $V_{G.d}$, and $V_{G.q}$.

As the PLL is supposed to align v_G on the q axis, $V_{G.d}$ will be zero in steady-state given that the PLL operates successfully, and also, $V_{G.q}$ will be equal to the magnitude of the grid voltage. Therefore, the value of $V_{G.q}$ could be used to detect voltage sag and swell. As shown in Fig. 5b, $V_{G,q}$ is compared to the nominal grid voltage magnitude ($V_{Lm,ref}$), so if $V_{G,q} \leq V_{Lm,ref} \times 0.9$ voltage sag will be detected and if $V_{G,q} \geq V_{Lm,ref} \times 1.1$, voltage swell will be detected. In case of any voltage sag or swell, the control circuit enables the DVR to compensate for the grid voltage.

As shown in Fig. 5b, to obtain the reference of the load voltage ($v_{L,ref}$), the normalized grid voltage ($v_{G,\alpha} / V_{G,q}$) and the reference value of the load voltage magnitude ($V_{L,ref}$) can be obtained as follows:

$$\frac{v_{G,\alpha}}{V_{G,q}} = \sin\ \omega t + \theta$$
$$V_{L,ref} = \frac{20000}{\sqrt{3}} \times \sqrt{2} = 16330 \tag{14}$$

So by multiplying $(v_{G,\alpha}/V_{G,q})$ and $(V_{L,ref})$, a reference voltage signal with a fixed nominal magnitude and in-phased with the grid voltage is obtained as (15):

$$\xrightarrow{(14)} v_{L,ref} = V_{L,ref} \times \frac{v_{G,\alpha}}{V_{G,q}} = 16330 \sin\ \omega t + \theta \tag{15}$$

Taking Fig. 3 into account, the converter output state equations are written as follows:

$$i_L = C\frac{dv_c}{dt} + ni_{out} \tag{16}$$

and

$$v_C = \pm D v_G - R i_L - L\frac{di_L}{dt}$$
$$\Rightarrow \frac{di_L}{dt} = -\frac{1}{L}v_C \pm \frac{1}{L}Dv_G - \frac{R}{L}i_L \tag{17}$$

where, L and C are the filter inductance and capacitance, respectively. Also, R is the equivalent resistance of the inductor.

Moreover, i_L is the filter inductor current, i_{out} is the load current.

Finally, n is the transformer turns ratio. Hereinafter n will be considered to be 1 (n=1). As (v_C) is the voltage on the output filter capacitor and the transformer turns ratio is n=1, it will be equal to the voltage on the transformer secondary side, i.e. it is the injected compensating voltage $(v_C = v_D)$.

In (17) the positive sign is for the voltage sag compensation and the minus sign is for the voltage swell compensation. According to (17), v_C that is equal to v_D, depends on the value of D, and according to (2), $v_L = v_G + v_D$, so if an error occurs in the output voltage (v_L), by using the combined feedback and feedforward control, the output voltage will be compensated and it is returned to the reference voltage $(v_{L,ref})$.

As shown in Fig. 5, for designing combined feedback and feed-forward control the following steps are taken.

A) For feedforward control, the v_{CFF} value, which is the difference between the reference voltage $(v_{L,ref})$ and the input voltage (v_G), is calculated according to (18):

$$v_{CFF} = v_{L,ref} - v_G \tag{18}$$

B) Feedback control (v_{CFB}) consists of two voltage errors:

1- the difference between the reference voltage and the output voltage $(v_{L,ref} - v_L)$, to eliminate the output error includes amplitude or harmonic errors in the output.

2- the difference between the input voltage (v_G) and filtered input voltage by QSG-PLL (v_α), to eliminate the harmonics on the grid.

$$v_{CFB} = (v_{L,ref} - v_L) + (v_G - v_\alpha) \tag{19}$$

C) After applying PI control on v_{CFB}, the sum of v_{CFB} and v_{CFF} is obtained and divided by v_G to obtain a value between 0 and 1, considering that their value is multiplied by (-1) in the swell mode. This value is denoted by D according to (20):

$$D = \frac{v_{CFB} + v_{CFF}}{v_G} \tag{20}$$

As shown in Fig. 5, the value of D that was obtained in (20), will be compared to a 10 kHz triangular waveform for creating a PWM waveform proportional to the amount of voltage sag, voltage swell, or harmonic fault. This PWM voltage is applied to the AC chopper and creates a waveform as shown in Fig. 4 and after being filtered by the LC low-pass filter, it is applied to the network in series through the injection transformer.

Results and Discussion

The effectiveness and feasibility of the proposed DVR with the proposed control system have been verified by simulations and experiments. For the simulation with MATLAB/Simulink software, a three-phase DVR installed in a three-phase 20kV distribution line is considered. Moreover, a scaled-down single-phase 220V prototype of the DVR is implemented that its results are presented and discussed.

A. Simulation Result

The simulation parameters are presented in Table 2.

Table 2: Simulation parameters 20kV three-phase DVR

Description	Symbol	Value
Grid rms line-line voltage	V_G	20 kV
Grid frequency	f	50 Hz
Series transformer ratio	n	1:1
Filters inductance	L	1 mH
Filters capacitance	C	22 µF
Filters resistance	R	1 Ω
Controller parameter (GPI)	K_p	1
Controller parameter (GPI)	K_i	0.7
Switching frequency	fs	10 kHz

For the first case, simulation of DVR performance to compensate for balanced three-phase voltage sag compensation is investigated. The simulation results of this case study are presented in Fig. 6. The grid voltage encounters 0.25pu voltage sag starting at t=0.12s and ends at t=0.2. Fig. 6a indicates the grid voltage in which the voltage sag occurrence is clear. As soon as the voltage sag is detected by the control system, the DVR operates to generate the required compensation voltage as shown in Fig. 5b. The DVR output voltage is added to the grid voltage so that the load voltage is restored to its nominal value which is indicated in Fig. 6c.

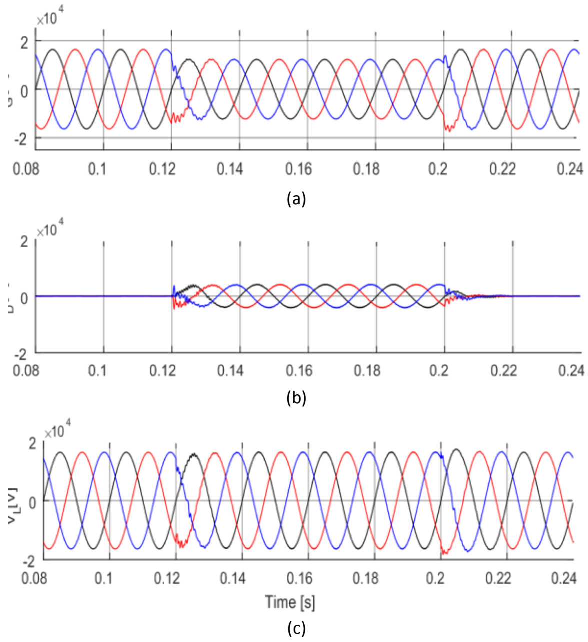

Fig. 6: Compensation of balanced voltage sag (0.25pu) (a) grid voltage, (b) injected voltage, (c) load voltage.

The performance of the DVR in compensating for balanced three-phase voltage swell is shown in Fig. 7. In this case, a 0.3pu balanced three-phase voltage swell is applied on the grid voltage which starts at t=0.12s and ends at t=0.2s. The DVR output voltage which is injected in series to the grid is shown in Fig. 7b. As the figure indicates, the DVR voltage is in the opposite phase with the grid voltage so that the voltage on the load side is reduced to the nominal value as illustrated in Fig. 7c.

According to the PQ $_{\text{monitored}}$ records, most of the voltage events in the three-phase systems are single-phase voltage sag in which one phase is affected. The next simulation case study is for single-phase voltage sag compensation. As Fig. 8a indicates, the grid voltage faces 0.45pu voltage on one of the phases which starts at t=0.12s and lasts for four fundamental cycles. The DVR output voltage, in this case, is shown in Fig. 8b. As this figure illustrates, the DVR generates the required compensating voltage in only the affected phase and injects it into the grid so that the voltage on the load side is a balanced three-phase voltage with nominal magnitude (Fig. 8c).

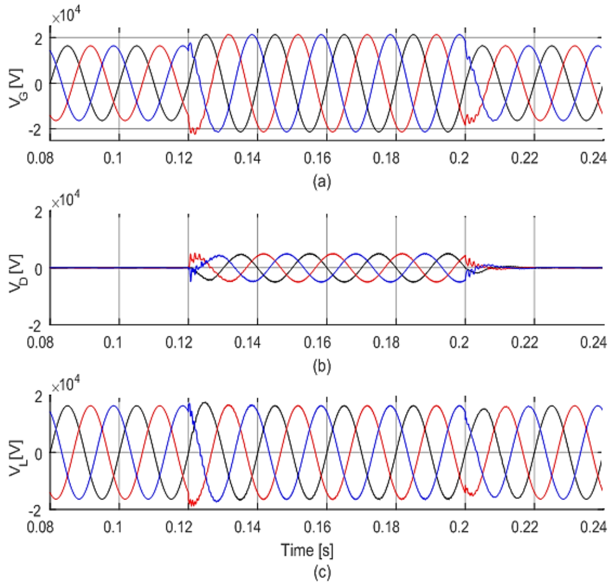

Fig. 7: Compensation for balanced three-phase voltage swell (0.3pu), (a) grid voltage, (b) injected voltage, (c) load voltage.

One of the important characteristics of the proposed control method is harmonic compensation. Fig. 9 shows concurrent harmonics and voltage sag compensation by about 12% of the THD and voltage sag of 0.3pu. Fig. 9b shown the DVR output voltage which is injected in series to the grid. The load voltage shown in Fig. 9c indicates that the harmonic compensation has been performed to an acceptable value and THD decreased to about 4.5%.

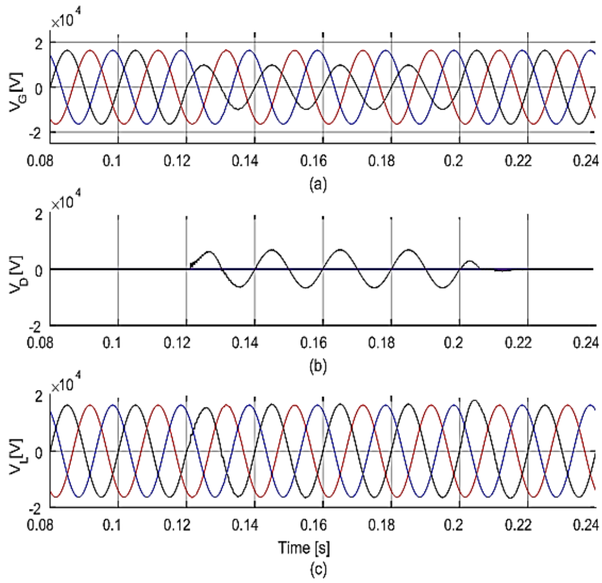

Fig. 8. Compensation of unbalanced voltage sag in phase a (0.4pu); (a) grid voltage, (b) injected voltage, (c) load voltage.

To compare the performance of CFBFFC with the PI control, both of the methods have been applied on the

DVR and the results are compared. For comparison, two important items are considered which the load voltage magnitude error are during the compensation and the other is the THD of the output voltage. The comparisons are indicated in Fig. 10. As the figure indicates, the load voltage error, as well as the THD of the DVR output voltage in the proposed CFBFFC, is considerably lower than the PI method which verifies the superiority of the CFBFFC in controlling the AC-AC converter-based DVR.

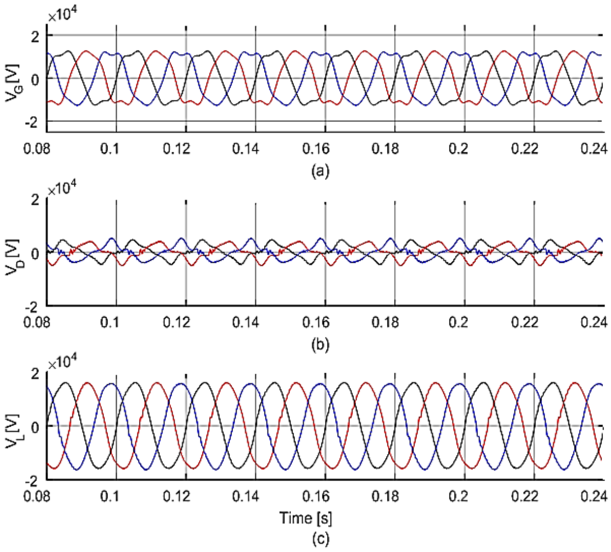

Fig. 9: Compensation of simultaneous harmonics and voltage sag fault (0.7 p.u); (a): grid voltage, (b): injected voltage, (c): load voltage.

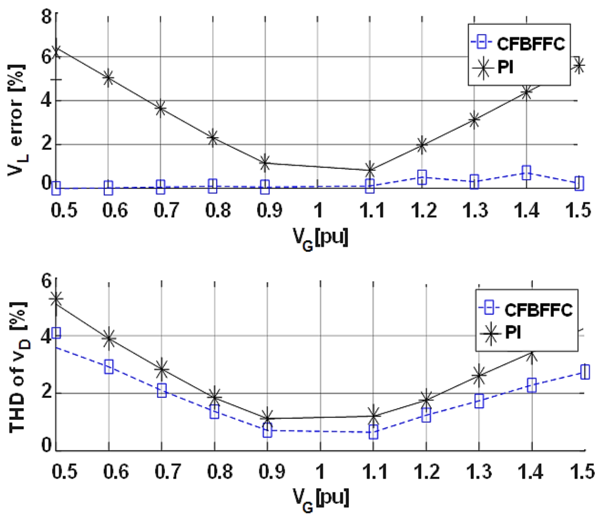

Fig. 10: Performance comparison of the CFBFFC and PI control methods in controlling the AC-AC converter-base DVR.

B. Experimental Result

As shown in Fig. 11, a scaled-down prototype of the proposed DVR is implemented and tested to verify its performance. For the experimental studies, a single-phase 220V DVR is implemented. In the implemented prototype, the FGH40N60SMD IGBTs are used. For realizing a bidirectional AC switch, two IGBTs are used in a common-emitter arrangement so that one switch driver is needed for each switch. Control signals are applied to IGBT switches via the DE2-70 FPGA board the input and output filter inductance is about 1mH and their capacitance is 2uF [30]. The switching frequency is selected to be 10 kHz. Table 3 shows the experimental parameters of single-phase DVR.

The experimental results for voltage sag compensation are indicated in Fig. 12 and Fig. 13. The grid voltage and load voltage are shown in Fig. 12a, in which about 0.45pu and 0.25pu the voltage sag occurred sequentially at the grid voltage, however, the load voltage is restored to its nominal condition. Fig. 12b shows the converter output voltage before and after the filter. In the place where the voltage amplitude is lower, with increasing duty cycle (D) the output amplitude of the converter is large enough to compensate for the output voltage properly.

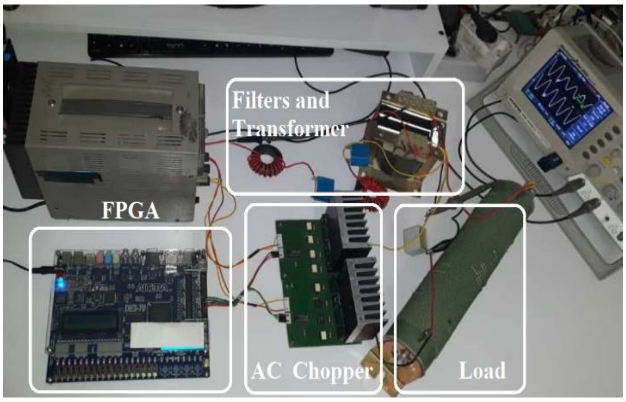

Fig. 11. Photo of the test set-up.

Table 3: Experimental parameters of single-phase DVR

Description	Symbol	Value	Unit
Grid voltage	V_G	**220**	V
Grid frequency	f	**50**	Hz
IGBT	FGH40N60SMD	**8**	-
FPGA Altera Board	DE2-70	**1**	-
Series transformer ratio	n	**1:1**	-
Filters inductance	L	**1**	mH
Filters capacitance	C	**22**	µF
Controller parameter (GPI)	K_p	**1**	-
Controller parameter (GPI)	K_i	**0.7**	-
Switching frequency	f_s	**10**	kHz

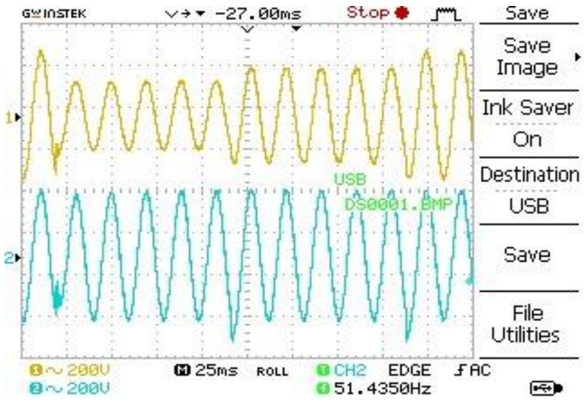

(a)

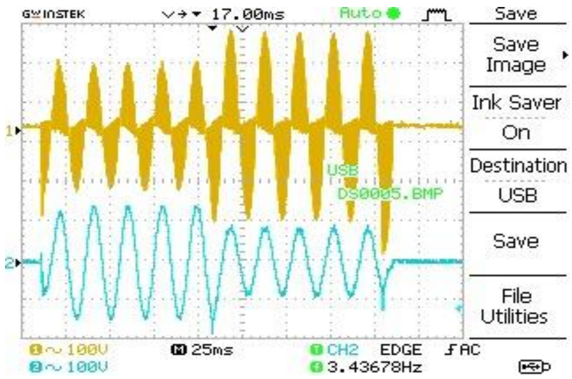

(b)

Fig. 12: Experimental results of voltage sag compensation, (a) grid voltage (upper) and load voltage, (b) converter output voltage before filter (upper), DVR output voltage.

Fig. 13a shows the grid current and the DVR input current and Fig. 13b shows the load current. As can be seen, the low current caused by the voltage sag is compensated by the DVR and the output current is stabilized.

The experimental results for voltage swell compensation are shown in Fig. 14 and Fig 15.

The grid voltage and load voltage are shown in Fig. 14a.

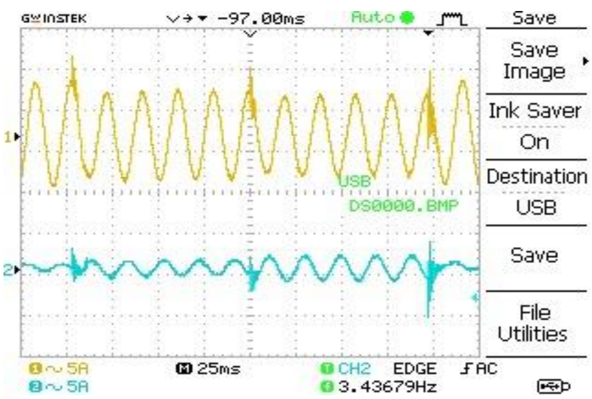

(a)

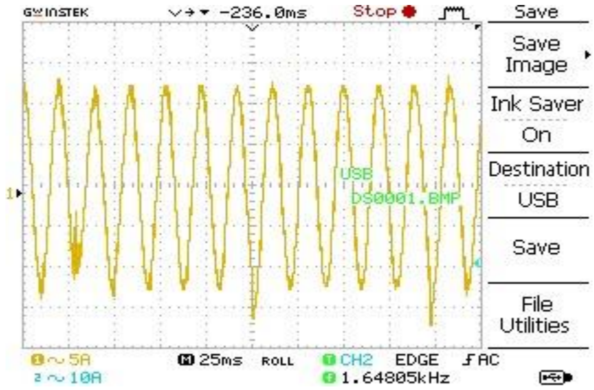

(b)

Fig. 13: Experimental results of voltage sag compensation, (a) grid current (upper) and the DVR input current (lower), (b)load current.

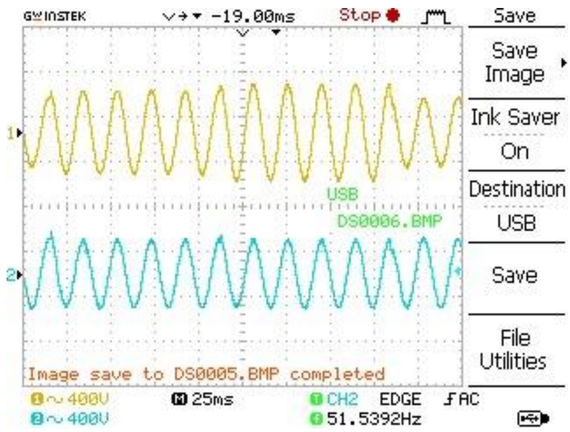

(a)

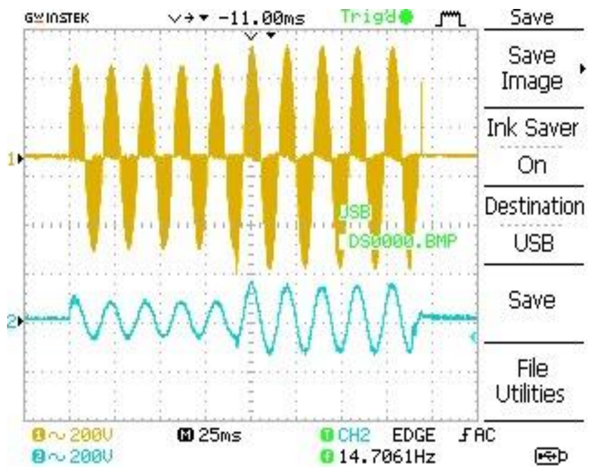

(b)

Fig. 14: Experimental results of voltage swell compensation, (a) grid voltage and load voltage, (b) converter output voltage before filter (upper), DVR output voltage.

As shown in the figure, 0.20pu and 0.40pu voltage swell occurred sequentially at the grid voltage, the DVR is placed in the circuit and compensates for the voltage by adding voltage in the opposite phase and returns the load voltage to its nominal state. Fig. 14b shows the converter output voltage which is a high-frequency PWM switched voltage waveform and the DVR output voltage.

In Fig. 15a for 0.40pu and 0.20pu voltage swell occurred sequentially shows the grid current and the DVR input current and Fig.15b shows the load current. As can be seen, the high current in the grid caused by the voltage swell is compensated by the DVR and the output current is stabilized.

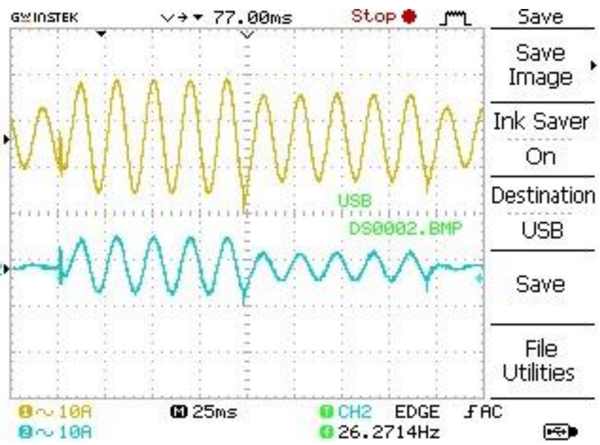

(a)

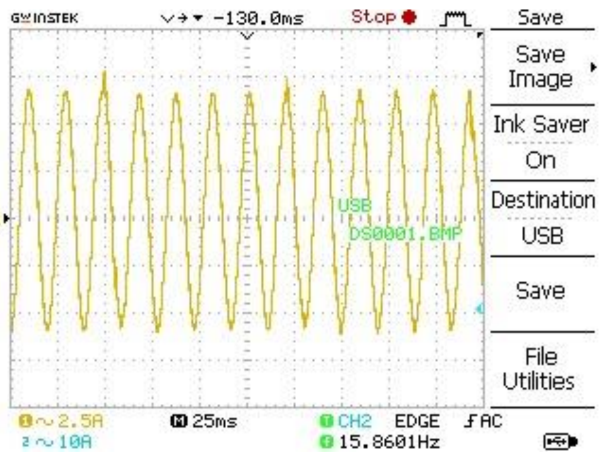

(b)

Fig. 15: Experimental results of voltage swell compensation, (a) grid current (upper) and the DVR input current (lower), (b)load current.

Conclusion

In this paper, a three-phase three-wire dynamic voltage restorer (DVR) was assessed using direct AC-AC converters without using a supply source and DC link. A control system based on combined feedback and feedforward control (CFBFFC) and SOGI-PLL has been proposed for the DVR. The CFBFFC has some intrinsic advantages such as high speed, low error, good response quality, and very simple implementation. Also, the SOGI-PLL extracts the phase angle and dq component of the voltage quickly and accurately which is necessary for the DVR control system.

The simulation results on a three-phase 20kV system as well as the experimental results obtained from a single-phase 220V system verified the performance of the DVR and the control system.

As the studies indicated, the adopted control system results in lower THD of the voltage waveforms and lower deviation (comparing the nominal value) in the load voltage magnitude in comparison with the conventional PI-based control methods. It was shown that this structure can compensate for up to 0.5pu voltage sag, up to above 1pu voltage swell, and all kinds of harmonic faults.

Author Contribution

H. Feshki Farahani and M. Asadi proposed and designed the structure of DVR and M. Farhadi-kangarlu proposed the control system. R. Nasrollahi, M. Farhadi-kangarlu, and P. Amiri implemented the experimental setup and designed the simulations and experiments. R. Nasrollahi collected the data and carried out the data analysis and wrote the original draft of the manuscript. H. Feshki Farahani and M. Asadi reviewed the data analysis and results as well as reviewed and edited the manuscript.

Acknowledgment

Special thanks to the Department of Electrical Engineering of the Islamic Azad University, Central Tehran Branch, as well as the judges and the editor of JECEI for their useful comments and suggestions.

Conflict of Interest

The authors declare no potential conflict of interest regarding the publication of this work. In addition, ethical issues including plagiarism, informed consent, misconduct, data fabrication and, or falsification, double publication and, or submission, and redundancy have been completely witnessed by the authors.

Abbreviations

DVR	Dynamic Voltage Restorer
PWM	Pulse- Width Modulation
CFBFFC	Combined Feedback and Feedforward Control
PLL	Phased-Locked-Loop
SOGI	Second Order Generalized Integrator
QSG	Quadrature Signal Generation

References

[1] P. Heine, M. Lehtonen, "Voltage sag distributions caused by power system faults," IEEE Trans. Power Syst., 18(4): 1367-1373, 2003.

[2] M.R. Islam, H. Lu, J. Hossain, L. Li, "Multiobjective optimization technique for mitigating unbalance and improving voltage considering higher penetration of electric vehicles and distributed generation," IEEE Syst. J., 14(3): 3677-3686, 2020.

[3] P.K. Ray, S.R. Das, A. Mohanty, "Fuzzy-controller-designed-PV-based custom power device for power quality enhancement," IEEE Trans. Energy Convers., 34(1): 405-414, 2018.

[4] S. Biricik, H. Komurcugil, "Optimized sliding mode control to maximize existence region for single-phase dynamic voltage restorers," IEEE Trans. Ind. Inf., 12(4): 1486-1497, 2016.

[5] G.S. Chawda, A.G. Shaik, O.P. Mahela, S. Padmanaban, J.B. Holm-Nielsen, "Comprehensive review of distributed facts control algorithms for power quality enhancement in utility grid with renewable energy penetration," IEEE Access, 8: 107614-107634, 2020.

[6] M.R. Khalid, M.S. Alam, A. Sarwar, M.J. Asghar, "A comprehensive review on electric vehicles charging infrastructures and their impacts on power-quality of the utility grid," eTransportation, 1: 100006, 2019.

[7] H.F. Farahani, "Improving voltage unbalance of low-voltage distribution networks using plug-in electric vehicles," J. Cleaner Prod., 148: 336-346, 2017.

[8] J.J. Paserba, G.F. Reed, M. Takeda, T. Aritsuka, "FACTS and custom power equipment for the enhancement of power transmission system performance and power quality," in Proc. SEPOPE Conference, 2000.

[9] H. Ribeiro, H. Marques, B.V. Borges, "Characterizing and monitoring voltage transients as problem to sensitive loads," Int. J. Electr. Power Energy Syst., 43(1): 1305-1317, 2012.

[10] C. Sundarabalan, K. Selvi, "Power quality enhancement in power distribution system using artificial intelligence based dynamic voltage restorer," Int. J. Electr. Eng. Inf., 5(4): 433, 2013.

[11] M. Elsaharty, J. Rocabert, J.I. Candela, P. Rodriguez, "Three-phase custom power active transformer for power flow control applications," IEEE Trans. Power Electron., 34(3): 2206-2219, 2018.

[12] J.A. Martinez, J. Martin-Arnedo, "Voltage sag studies in distribution networks-part II: Voltage sag assessment," IEEE Trans. Power Delivery, 21(3): 1679-1688, 2006.

[13] F.M. Mahdianpoor, R.A. Hooshmand, M. Ataei, "A new approach to multifunctional dynamic voltage restorer implementation for emergency control in distribution systems," IEEE Trans. Power Delivery, 26(2): 882-890, 2011.

[14] R. Pal, S. Gupta, "Topologies and control strategies implicated in dynamic voltage restorer (DVR) for power quality improvement," Iran. J. Sci. Technol. Trans. Electr. Eng, 44: 581-603, 2020.

[15] M. Farhadi-Kangarlu, E. Babaei, F. Blaabjerg, "A comprehensive review of dynamic voltage restorers," Int. J. Electr. Power & Energy Sys., 92: 136-155, 2017.

[16] P. Szczesniak, "Challenges and design requirements for industrial applications of AC/AC power converters without DC-link," Energies, 12(8): 1581, 2019.

[17] M. Banaei, S. Hosseini, M.D. Khajee, "Mitigation of voltage sag using adaptive neural network with dynamic voltage restorer," in Proc. 2006 CES/IEEE 5th International Power Electronics and Motion Control Conference, 2: 1-5, 2006.

[18] C. Kumar, M.K. Mishra, "Predictive voltage control of transformerless dynamic voltage restorer," IEEE Trans. Ind. Electron., 62(5): 2693-2697, 2014.

[19] B. Ferdi, C. Benachaiba, S. Dib, R. Dehini, "Adaptive PI control of dynamic voltage restorer using fuzzy logic," J. Electr. Eng. Theor. Appl., 1(3): 165-173, 2010.

[20] P. Roncero-Sanchez, E. Acha, "Dynamic voltage restorer based on flying capacitor multilevel converters operated by repetitive control," IEEE Trans. Power Delivery, 24(2): 951-960, 2009.

[21] H. Komurcugil, S. Biricik, E. Babaei, "Super twisting algorithm based sliding mode control method for single-phase dynamic voltage restorers," in Proc. 2019 2nd International Conference on Smart Grid and Renewable Energy (SGRE): 1-6, 2019.

[22] L.P. Vasudevan, V. Prasad, "Performance enhancement of a dynamic voltage restorer," Turk. J. Electr. Eng. Comput. Sci., 25(3): 2293-2307, 2017.

[23] E. Babaei, M.F. Kangarlu, "Sensitive load voltage compensation against voltage sags/swells and harmonics in the grid voltage and limit downstream fault currents using DVR," Electr. Power Syst. Res., 83(1): 80-90, 2012.

[24] A. Koerbe, R. King, "Combined feedback–feedforward control of wind turbines using state-constrained model predictive control," IEEE Trans. Control Syst. Technol., 21(4): 1117-1128, 2013.

[25] M.T. Yan, Y.J. Shiu, "Theory and application of a combined feedback–feedforward control and disturbance observer in linear motor drive wire-EDM machines," Int. J. Mach. Tools Manuf. , 48(3-4): 388-401, 2008.

[26] J. Perez, V. Cárdenas, L. Moran, C. Núñez, "Single-phase ac-ac converter operating as a dynamic voltage restorer (DVR)," in Proc. IECON 2006-32nd Annual Conference on IEEE Industrial Electronics: 1938-1943, 2006.

[27] M. Farhadi Kangarlu, E. Babaei, F. Blaabjerg, "An LCL-filtered single-phase multilevel inverter for grid integration of PV systems," J. Oper. Autom. Power Eng., 4(1): 54-65, 2016.

[28] J. Matas, M. Castilla, L.G. De Vicuña, J. Miret, J.C. Vasquez, "Virtual impedance loop for droop-controlled single-phase parallel inverters using a second-order general-integrator scheme," IEEE Trans. Power Electron., 25(12): 2993-3002, 2010.

[29] M. Farhadi-Kangarlu, F. Mohammadi, "Performance improvement of single-phase transformerless grid-connected PV inverters regarding common-mode voltage (CMV) and LVRT," J. Oper. Autom. Power Eng., 7(1): 1-15, 2019.

[30] A.M. Khiavi, J. Sobhi, Z.D. Koozehkanani, M.F. Kangarlu, "FPGA-based reconfigurable PWM generator for power electronic converter applications," J. Oper. Autom. Power Eng., 28(4): 516-531, 2017.

Biographies

Reza Nasrollahi was born in Boukan, Iran in 1976. He received B.Sc. degree in Technical teaching in Electrical-Electronic from Shahid Rajaee Teacher Training University, Tehran, Iran, in 2001, the M.Sc. degree in Electrical Engineering in 2007 from the University of Urmia, Urmia, Iran. Currently, He is Ph.D. student in Electrical Engineering at the Islamic Azad University Central Tehran Branch, Tehran, Iran. His research interests include power quality, power-electronic converters, renewable energy systems as well as digital and analog microelectronics.

Hassan Feshki Farahani received his B.Sc. degree in Electrical Engineering from Shahed University in 2002, M.Sc degree from Iran University of Science & Technology (IUST) in Electrical Engineering, in 2005 and Ph.D. degree in Electrical Engineering from, Science & Research Branch, Islamic Azad University, Tehran, Iran in 2012. Currently, he is an Associate Professor at the Department of Engineering, Islamic Azad University, Ashtian Branch, Ashtian, Iran, and also Central Tehran Branch, Islamic Azad University, Tehran, Iran. His special fields of interest include electric vehicles, power electronics, smart grids, and electricity markets.

Mehdi Asadi received the B.Sc., M.Sc., and Ph.D. degrees in electrical engineering from Iran University of Science and Technology (IUST), Tehran, Iran in 2002, 2004, and 2013, respectively. He is currently working with Arak University of Technology, Arak, Iran. His research interests include power electronics, power quality, and electrical machine drives.

Mohammad Farhadi-Kangarlu was born in Kangarlu, East Azarbaijan, Iran, in 1987. He received the B.Sc., M.Sc. and Ph.D. degrees (first class Hons.) all in electric power engineering from the University of Tabriz, Tabriz, Iran, in 2008 and 2010, and 2014, respectively. His research interests include power electronic converters analysis and design, renewable energy systems, and power quality. He elevated to IEEE Senior Member grade in 2021. He has published more than 80 research papers, registered 9 patents, and co-authored a book. He joined the Faculty of Electrical and Computer Engineering, Urmia University, Iran in September 2014, where he currently holds the position of Associate Professor in power electronics.

Parviz Amiri received his Ph.D. from University Tarbiat Modares (TMU, Tehran, Iran) in 2010, all degrees in Electrical Engineering (electronic). His main research interest includes electronic circuit design in industries. His primary research interest is in RF and power electronic circuits, with a focus on highly efficient and high linear power circuit design. He is currently with the Faculty of Electrical Engineering at Shahid Rajaee Teacher Training University, Tehran, Iran.

How to cite this paper:

R. Nasrollahi, H. Feshki Farahani, M. Asadi, M. Farhadi-kangarlu, P. Amiri, “A SOGI-PLL-based feedback-feedforward control system for three-phase dynamic voltage restorer in the distribution grid,” J. Electr. Comput. Eng. Innovations, 10(1): 89-100, 2022.

DOI: 10.22061/JECEI.2021.7942.457

URL: https://jecei.sru.ac.ir/article_1566.html